Competition Between Synaptic Depression and Facilitation in Attractor Neural Networks

J. J. Torres
jtorres@onsager.ugr.es
Institute Carlos I for Theoretical and Computational Physics, and Department of Electromagnetism and Matter Physics, University of Granada, Granada E-18071, Spain

J. M. Cortes
jesus.m.cortes@gmail.com
Institute Carlos I for Theoretical and Computational Physics, and Department of Electromagnetism and Matter Physics, University of Granada, Granada E-18071, Spain, and Department of Physics, Radboud University of Nijmegen, 6525 EZ Nijmegen, Netherlands

J. Marro
jmarro@ugr.es
Institute Carlos I for Theoretical and Computational Physics, and Department of Electromagnetism and Matter Physics, University of Granada, Granada E-18071, Spain

H. J. Kappen
B.Kappen@science.ru.nl
Department of Medical Physics and Biophysics, Radboud University of Nijmegen, 6525 EZ Nijmegen, Netherlands

We study the effect of competition between short-term synaptic depression and facilitation on the dynamic properties of attractor neural networks, using Monte Carlo simulation and a mean-field analysis. Depending on the balance of depression, facilitation, and the underlying noise, the network displays different behaviors, including associative memory and switching of activity between different attractors. We conclude that synaptic facilitation enhances the attractor instability in a way that (1) intensifies the system adaptability to external stimuli, which is in agreement with experiments, and (2) favors the retrieval of information with less error during short time intervals.

The current address for J. M. Cortes is Institute for Adaptive and Neural Computation, School of Informatics, University of Edinburgh, Edinburgh, EHI 2QL, U.K.

1 Introduction and Model

Recurrent neural networks are a prominent model for information processing and memory in the brain (Hopfield, 1982; Amit, 1989). Traditionally, these models assume synapses that may change on the timescale of learning but that can be assumed constant during memory retrieval. However, synapses are reported to exhibit rapid time variations, and it is likely that this finding has important implications for our understanding of the way information is processed in the brain (Abbott & Regehr, 2004). For instance, Hopfield-like networks in which synapses undergo rather generic fluctuations have been shown to significantly improve the associative process (Marro, Garrido, & Torres, 1998). In addition, motivated by specific neurobiological observations and their theoretical interpretation (Tsodyks, Pawelzik, & Markram, 1998), activity-dependent synaptic changes that induce depression of the response have been considered (Pantic, Torres, Kappen, & Gielen, 2002; Bibitchkov, Herrmann, & Geisel, 2002). It was shown that synaptic depression induces, in addition to memories as stable attractors, special sensitivity of the network to changing stimuli as well as rapid switching of the activity among the stored patterns (Pantic et al., 2002; Cortes, Garrido, Marro, & Torres, 2004; Marro, Torres, & Cortes, 2007; Torres et al., 2005; Cortes, Torres, Marro, Garrido, & Kappen, 2006). This behavior has been observed experimentally to occur during the processing of sensory information (Laurent et al., 2001; Mazor & Laurent, 2005; Marro, Torres, Cortes, & Wemmenhove, 2006).

In this letter, we present and study networks that are inspired in the observation of certain more complex synaptic changes. That is, we assume that repeated presynaptic activation induces at short times not only depression but also facilitation of the postsynaptic potential (Thomson & Deuchars, 1994; Zucker & Regehr, 2002; Burnashev & Rozov, 2005; Wang et al., 2006). The question, which has not been quite addressed yet, is how competition between depression and facilitation will affect network performance. We here conclude that as for the case of only depression (Pantic et al., 2002; Cortes et al., 2006), the system may exhibit up to three different phases or regimes: one with standard associative memory, a disordered phase in which the network lacks this property, and an oscillatory phase in which activity switches between different memories. Depending on the balance between facilitation and depression, novel intriguing behavior results in the oscillatory regime. In particular, as the degree of facilitation increases, the sensitivity to external stimuli is enhanced and the frequency of the oscillations increases. It then follows that facilitation allows recovering of information with less error, at least during a short interval of time, and can therefore play an important role in short-term memory processes. We are concerned here with a network of binary neurons. Previous studies have shown that the behavior of such a simple network dynamics agrees qualitatively with the behavior that is observed in more realistic networks,

such as integrate-and-fire neuron models of pyramidal cells (Pantic et al., 2002).

Let us consider N binary neurons, $s_i = \{1, 0\}$, $i = 1, \ldots, N$, endowed with probabilistic dynamics,

$$\text{Prob}\{s_i(t + 1) = 1\} = \frac{1}{2}\{1 + \tanh[2\beta h_i(t)]\}, \tag{1.1}$$

which is controlled by a temperature parameter, $T \equiv 1/\beta$ (see, e.g., Peretto, 1992; Marro & Dickman, 2005), for details. The function $h_i(t)$ denotes a time-dependent local field, that is, the total presynaptic current arriving at the postsynaptic neuron i. This will be determined in the model following the phenomenological description of nonlinear synapses reported in Markram, Wang, and Tsodyks (1998) and Tsodyks et al. (1998), which was shown to capture well the experimentally observed properties of neocortical connections. Accordingly, we assume that

$$h_i(t) = \sum_{j=1}^{N} \omega_{ij} \mathcal{D}_j(t) \mathcal{F}_j(t) s_j(t) - \theta_i, \tag{1.2}$$

where θ_i is a constant threshold associated with the firing of neuron i, and $\mathcal{D}_j(t)$ and $\mathcal{F}_j(t)$ are functions—to be determined—that describe the effect on the neuron activity of short-term synaptic depression and facilitation, respectively. We further assume that the weight ω_{ij} of the connection between the (presynaptic) neuron j and the (postsynaptic) neuron i are static and store a set of patterns of the network activity, namely, the familiar covariance rule:

$$\omega_{ij} = \frac{1}{Nf(1 - f)} \sum_{\nu=1}^{P} (\xi_i^\nu - f)(\xi_j^\nu - f). \tag{1.3}$$

Here, $\xi^\nu = \{\xi_i^\nu\}$, with $\nu = 1 \ldots, P$, are different binary patterns of average activity $\langle \xi_i^\nu \rangle \equiv f$. The standard Hopfield model is recovered for $\mathcal{F}_j = \mathcal{D}_j = 1, \forall j = 1, \ldots, N$.

We next implement a dynamics for $\mathcal{F}_j$ and $\mathcal{D}_j$ after the prescription in Markram et al. (1998) and Tsodyks et al. (1998). A description of varying synapses requires at least three local variables, say, $x_j(t)$, $y_j(t)$, and $z_j(t)$, to be associated to the fractions of neurotransmitters in recovered, active, and inactive states, respectively. A simpler picture consists in dealing with only the $x_j(t)$ variable. This simplification, which seems to describe accurately both interpyramidal and pyramidal interneuron synapses, corresponds to the fact that the time in which the postsynaptic current decay is much shorter than the recovery time for synaptic depression, say, τ_{rec} (Markram

& Tsodyks, 1996) (time intervals are in milliseconds hereafter). Within this approach, one may write that

$$x_j(t+1) = x_j(t) + \frac{1 - x_j(t)}{\tau_{\text{rec}}} - \mathcal{D}_j(t)\mathcal{F}_j(t)s_j(t), \tag{1.4}$$

where

$$\mathcal{D}_j(t) = x_j(t) \tag{1.5}$$

and

$$\mathcal{F}_j(t) = U + (1 - U)\, u_j(t). \tag{1.6}$$

The interpretation of this ansatz is as follows. Concerning any presynaptic neuron j, the product $\mathcal{D}_j\mathcal{F}_j$ stands for the total fraction of neurotransmitters in the recovered state that are activated by either incoming spikes, $U_j x_j$, or facilitation mechanisms, $(1 - U_j)x_j u_j$; for simplicity, we are assuming that $U_j = U \in [0, 1]\, \forall j$. The additional variable $u_j(t)$ is assumed to satisfy, as in the quantal model of transmitter release in Markram et al. (1998), that

$$u_j(t+1) = u_j(t) - \frac{u_j(t)}{\tau_{\text{fac}}} + U[1 - u_j(t)]s_j(t), \tag{1.7}$$

which describes an increase with each presynaptic spike and a decay to the resting value with relaxation time τ_{fac}. Consequently, facilitation washes out ($u_j \to 0$, $F_j \to U$) as $\tau_{\text{fac}} \to 0$, and each presynaptic spike uses a fraction U of the available resources $x_j(t)$. The effect of facilitation increases with decreasing U, because this will leave more neurotransmitters available to be activated by facilitation. Therefore, facilitation is controlled not only by τ_{fac} but also by U.

The Hopfield case with static synapses is recovered after using $x_j = 1$ in equation 1.5 and $u_j = 0$ in equation 1.6 or, equivalently, $\tau_{\text{rec}} = \tau_{\text{fac}} = 0$ in equations 1.4 and 1.7. In fact, the latter imply fields $h_i(t) = \sum_j \omega_{ij} U s_j(t) - \theta_i$, so that one may simply rescale both β and the threshold.

The above interesting phenomenological description of dynamic changes has already been implemented in attractor neural networks (Bibitchkov et al., 2002; Pantic et al., 2002) for pure depressing synapses between excitatory pyramidal neurons (Tsodyks & Markram, 1997). We are interested here in the consequences of a competition between depression and facilitation. Therefore, we shall use T, U, τ_{rec}, and τ_{fac} in the following as relevant control parameters.

2 Mean-Field Solution

Let us consider the mean activities associated, respectively, with active and inert neurons in a given pattern v:

$$m_+^v(t) \equiv \frac{1}{Nf} \sum_{j \in \text{Act}(v)} s_j(t), \quad m_-^v(t) \equiv \frac{1}{N(1-f)} \sum_{j \notin \text{Act}(v)} s_j(t). \qquad (2.1)$$

It follows for the overlap of the network activity with pattern v that

$$m^v(t) \equiv \frac{1}{Nf(1-f)} \sum_i \left(\xi_i^v - f\right) s_i(t) = m_+^v(t) - m_-^v(t), \qquad (2.2)$$

$\forall v$. One may also define the averages of x_i and u_i over the sites that are active and inert, respectively, in a given pattern v:

$$x_+^v(t) \equiv \frac{1}{Nf} \sum_{j \in \text{Act}(v)} x_j(t), \quad x_-^v(t) \equiv \frac{1}{N(1-f)} \sum_{j \notin \text{Act}(v)} x_j(t)$$

$$u_+^v(t) \equiv \frac{1}{Nf} \sum_{j \in \text{Act}(v)} u_j(t), \quad u_-^v(t) \equiv \frac{1}{N(1-f)} \sum_{j \notin \text{Act}(v)} u_j(t), \qquad (2.3)$$

$\forall v$, which describe depression (the xs) and facilitation (the us), each concerning a subset of neurons, for examples, $N/2$ neurons for $f = 1/2$.

One may solve the model, equations 1.1 to 1.7, in the thermodynamic limit $N \to \infty$ under the standard mean-field assumption that $s_i \approx \langle s_i \rangle$. This type of approach has recently been reported to satisfactorily explain the behavior of recurrent networks of spiking neurons with short-term depressing synapses (Romani, Amit, & Mongillo, 2006). Here, within this approximation, we shall substitute x_i (u_i) by the mean-field values $x_\pm^v$ ($u_\pm^v$) (notice that one expects, and it will be confirmed below by comparisons with direct simulation results, that the mean-field approximation is accurate away from any possible critical point). The local fields then ensue as

$$h_i(t) = \sum_{v=1}^{P} \left(\xi_i^v - f\right) M^v(t), \qquad (2.4)$$

$$M^v(t) \equiv \left[U + (1-U)\, u_+^v(t)\right] x_+^v(t) m_+^v(t) - \left[U - (1-U)\, u_-^v(t)\right] x_-^v(t) m_-^v(t).$$

Assuming further that patterns are random with mean activity $f = 1/2$, one obtains the set of dynamic equations:

$$x_{\pm}^{\nu}(t+1) = x_{\pm}^{\nu}(t) + \frac{1 - x_{\pm}^{\nu}(t)}{\tau_{\text{rec}}} - \left[U + (1 - U)\, u_{\pm}^{\nu}(t) \right] x_{\pm}^{\nu}(t)\, m_{\pm}^{\nu}(t),$$

$$u_{\pm}^{\nu}(t+1) = u_{\pm}^{\nu}(t) - \frac{u_{\pm}^{\nu}(t)}{\tau_{\text{fac}}} + U \left[1 - u_{\pm}^{\nu}(t) \right] m_{\pm}^{\nu}(t),$$

$$m_{\pm}^{\nu}(t+1) = \frac{1}{N} \sum_i \left\{ 1 \pm \tanh\left(\beta \left[M^{\nu}(t) \pm \sum_{\mu \neq \nu} \epsilon_i^{\mu} M^{\mu}(t) \right] \right) \right\},$$

$$m^{\nu}(t+1) = \frac{1}{N} \sum_i \epsilon_i^{\nu} \tanh\left[\beta \sum_{\mu} \epsilon_i^{\mu} M^{\mu}(t) \right], \tag{2.5}$$

where $\epsilon_i^{\mu} \equiv 2\xi_i^{\mu} - 1$. This is a $6P$-dimensional coupled map whose analytical treatment is difficult for large P, but it may be integrated numerically, at least for not too large P. One may also find the fixed-point equations for the coupled dynamics of neurons and synapses; these are

$$x_{\pm}^{\nu} = \left\{ 1 + \left[U + (1 - U)\, u_{\pm}^{\nu} \right] \tau_{\text{rec}}\, m_{\pm}^{\nu} \right\}^{-1},$$

$$u_{\pm}^{\nu} = U\, \tau_{\text{fac}}\, m_{\pm}^{\nu} \left(1 + U\, \tau_{\text{fac}}\, m_{\pm}^{\nu} \right)^{-1},$$

$$2m_{\pm}^{\nu} = 1 \pm \frac{2}{N} \sum_i \tanh\left[\beta \left(M^{\nu} \pm \sum_{\mu \neq \nu} \epsilon_i^{\mu} M^{\mu} \right) \right],$$

$$m^{\nu} = \frac{1}{N} \sum_i \epsilon_i^{\nu} \tanh\left(\beta \sum_{\mu} \epsilon_i^{\mu} M^{\mu} \right). \tag{2.6}$$

The numerical solution of these transcendental equations describes the resulting order as a function of the relevant parameters. Determining the stability of these solutions for $\alpha = P/N \neq 0$ is a more difficult task, because it requires linearizing equation 2.5, and the dimensionality diverges in the thermodynamical limit (see, however, Torres, Pantic, & Kappen, 2002). In the next section, we therefore deal with the case $\alpha \to 0$.

3 Main Results

Consider a finite number of stored patterns P, that is, $\alpha = P/N \to 0$ in the thermodynamic limit. In practice, it is sufficient to deal with $P = 1$ to illustrate the main results (therefore, we suppress the index ν hereafter).

Let us define the vectors of order parameters $\vec{y} \equiv (m_+, m_-, x_+, x_-, u_+, u_-)$, its stationary value $\vec{y}_{st}$ that is given by the solution equation 2.6, and $\vec{F}$ whose components are the functions on the right-hand side of equation 2.5. The stability of equation 2.5 around the steady state of equation 2.6 follows from the first derivative matrix $D \equiv (\partial \vec{F} / \partial \vec{y})_{\vec{y}_{st}}$. This is

$$D = \begin{pmatrix} \bar{\beta} A_+ & -\bar{\beta} A_- & \bar{\beta} B_+ & -\bar{\beta} B_- & \bar{\beta} C_+ & -\bar{\beta} C_- \\ -\bar{\beta} A_+ & \bar{\beta} A_- & -\bar{\beta} B_+ & \bar{\beta} B_- & -\bar{\beta} C_+ & \bar{\beta} C_- \\ -A_+ & 0 & \tau - B_+ & 0 & -C_+ & 0 \\ 0 & -A_- & 0 & \tau - B_- & 0 & -C_- \\ D_+ & 0 & 0 & 0 & \tau - E_+ & 0 \\ 0 & D_- & 0 & 0 & 0 & \tau - E_- \end{pmatrix}, \quad (3.1)$$

where $\bar{\beta} \equiv 2\beta m_+ m_-$, $A_\pm \equiv [U + (1 - U) u_\pm] x_\pm$, $B_\pm \equiv [U + (1 - U) u_\pm] m_\pm$, $C_\pm \equiv (1 - U) x_\pm m_\pm$, $D_\pm \equiv U(1 - u_\pm)$, $\tau \equiv 1 - \tau_{rec}^{-1}$, and $E_\pm \equiv U m_\pm$. After noticing that $m_+ + m_- = 1$, one may numerically diagonalize D and obtain the eigenvalues λ_n for a given set of control parameters $T, U, \tau_{rec}, \tau_{fac}$. For $|\lambda_n| < 1$ ($|\lambda_n| > 1$), system is stable (unstable) close to the fixed point y_n. The maximum of $|\lambda_n|$ determines the local stability: for $|\lambda_n|_{max} < 1$, system 2.5 is locally stable, while for $|\lambda_n|_{max} > 1$, there is at least one direction of instability, and the system consequently becomes locally unstable. Therefore, varying the control parameters, one crosses the line $|\lambda|_{max} = 1$ that signals the bifurcation points.

The resulting situation is summarized in Figure 1 for specific values of $U, T,$ and τ_{fac}. Equations 2.6 have three solutions, two of which are memory states corresponding to the pattern and antipattern and the other a so-called paramagnetic state that has no overlap with the memory pattern. The stability of the two solutions depends on τ_{rec}. The region $\tau_{rec} > \tau_{rec}^{**}$ corresponds to the nonretrieval phase, where the paramagnetic solution is stable and the memory solutions are unstable. In this phase, the average network behavior has no significant overlap with the stored memory pattern. The region $\tau_{rec} < \tau_{rec}^{*}$ corresponds to the memory phase, where the paramagnetic solution is unstable and the memory solutions are stable. The network retrieves one of the stored memory patterns. For $\tau_{rec}^{*} < \tau_{rec} < \tau_{rec}^{**}$ (denoted O in the figure), none of the solutions is stable. The activity of the network in this regime keeps moving from one to the other fixed points neighborhood (the pattern and antipattern in this simple example). This rapid switching behavior is typical for dynamic synapses and does not occur for static synapses. A similar oscillatory behavior was reported in Pantic et al. (2002) and Cortes et al. (2004) for the case of only synaptic depression. A main novelty is that the inclusion of facilitation importantly modifies the phase diagram, as discussed below (see Figure 2). On the other hand, the phases for $\tau_{rec} < \tau_{rec}^{*}$ (F) and $\tau_{rec} > \tau_{rec}^{**}$ (P) correspond, respectively, to a locally
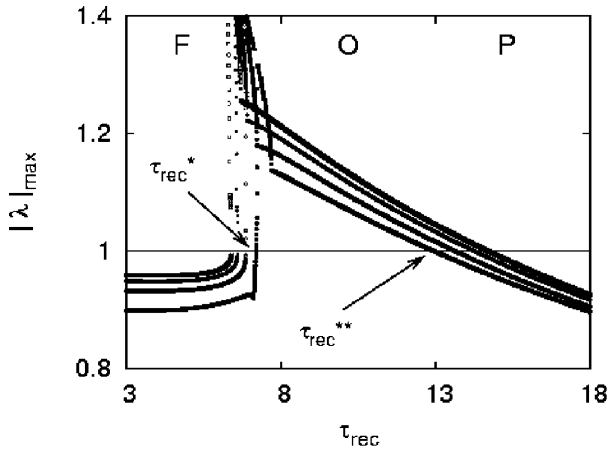
Figure 1: The three relevant regions, denoted F, O, and P, respectively, that are depicted by the absolute value of the maximum eigenvalue $|\lambda_n|_{max}$ of the stability matrix D in equation 3.1 when plotted as a function of the recovering time τ_{rec} for different values of the facilitation time τ_{fac}. Here, $\tau_{fac} = 10, 15, 20,$ and 25 for different curves from bottom to top, respectively, in the F and P regions. The stationary solutions lack any local stability for $\tau_{rec}^* < \tau_{rec} < \tau_{rec}^{**}$ (O), and the network activity then undergoes oscillations. The arrows signal τ_{rec}^* and τ_{rec}^{**} for $\tau_{fac} = 10$. This graph is for $U = 0.1$ and $T = 0.1$.

stable regime with associative memory ($m \neq 0$) and a disordered regime without memory ($m \equiv m^1 = 0$).

The values τ_{rec}^* and τ_{rec}^{**}, which, as a function of τ_{fac}, U and T, determine the limits of the oscillatory phase, correspond to the onset of condition $|\lambda_n|_{max} > 1$. This condition defines lines in the parameter space (τ_{rec}, τ_{fac}) that are illustrated in Figure 2. This reveals that for a relatively large degree of facilitation, τ_{rec}^* (separation between the F and O regions) in general decreases with increasing facilitation, which implies a larger oscillatory region and consequently a reduction of the memory phase. This is due to the additional depressing effect produced by strong facilitation, which tends to destabilize the ferromagnetic solutions. On the other hand, τ_{rec}^{**} (separation between O and P regions) in general increases with facilitation, thus broadening further the width of the oscillatory phase $\delta \equiv \tau_{rec}^{**} - \tau_{rec}^*$. Moreover, for relatively small facilitation, the behavior is more complex due to the balance between depression and facilitation. The width of the oscillatory phase thus increases when depression is dominant and decreases when facilitation becomes more important. At this regime, there is a competition between the tendency to stabilize ferromagnetic solutions due to facilitation and the opposite one due to depression, which results in a nonmonotonic behavior of δ. The behavior of δ under different conditions is illustrated in the insets
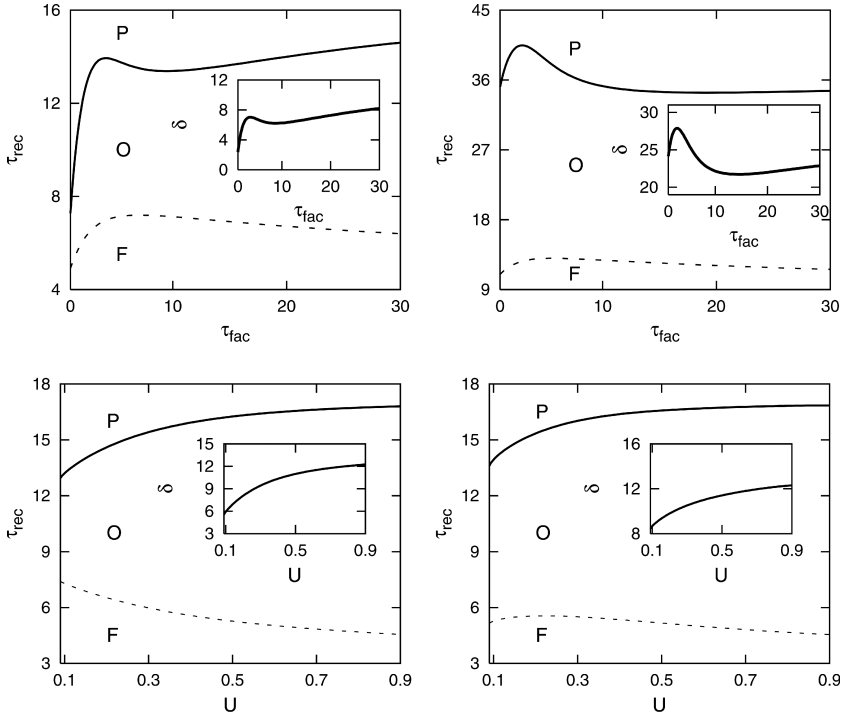
Figure 2: This illustrates how the different regimes of the network activity depend on the balance between depression and facilitation. (Top graphs) Phase diagram ($\tau_{\rm rec}$, $\tau_{\rm fac}$) for $\alpha = 0$ and $U = 0.1$ at temperature $T = 0.1$ (left) and 0.05 (right). The dashed (solid) line is for $\tau_{\rm rec}^{*}$ ($\tau_{\rm rec}^{**}$), signaling the first-order (second-order) phase transitions between the O and F(P) phases. The insets show the resulting width of the oscillatory region, $\delta \equiv \tau_{\rm rec}^{**} - \tau_{\rm rec}^{*}$, as a function of $\tau_{\rm fac}$. (Bottom graphs) Phase diagram ($\tau_{\rm rec}$, U) for $\alpha = 0$ and $T = 0.1$, and $\gamma \equiv \tau_{\rm fac}/\tau_{\rm rec} = 1$ (left) and 0.25 (right).

of Figure 2. These insets also show that the effects just described are more evident for low levels of noise (e.g., δ is larger for smaller temperature).

Also interesting is that facilitation induces changes in the phase diagram as one varies the facilitation parameter U, which measures the fraction of neurotransmitters not activated by the facilitating mechanism. In order to discuss this, we define the ratio between the timescales, $\gamma \equiv \tau_{\rm fac}/\tau_{\rm rec}$, and monitor the phase diagram ($\tau_{\rm rec}$, U) for varying γ. The result is also in Figure 2; see the bottom graphs for $\gamma = 1$ (left) and 0.25 (right), which correspond, respectively, to a situation in which depression and facilitation occur in the same timescale and a situation in which facilitation is four times faster. The two cases exhibit a similar behavior for large U, but they
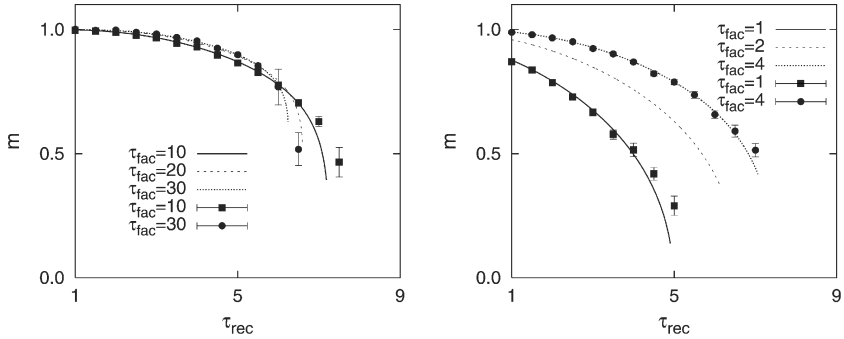
Figure 3: For $U = T = 0.1$ as in Figure 1, these graphs illustrate results from Monte Carlo simulations (symbols) and mean-field solutions (curves) for the case of associative memory under competition of depression and facilitation. This shows $m \equiv m^1$ as a function of τ_{rec} (horizontal axis) and τ_{fac} (different curves as indicated) corresponding to regimes in which the limiting value τ_{rec}^* decreases (left graph) or increases (right graph) with increasing τ_{fac}, the two situations discussed in the text.

are qualitatively different for small U. In the case of faster facilitation, there is a range of U values for which τ_{rec}^* increases in such a way that one passes from the oscillatory to the memory phase by slightly increasing U. This means that facilitation tries to drive the network activity to one of the attractors ($\tau_{fac} < \tau_{rec}$), and for weak depression (U small), the activity will remain there. Decreasing U further then has the effect of increasing effectively the system temperature, which destabilizes the attractor. This requires only small U because the dynamics 1.7 rapidly decreases the second term in $\mathcal{F}_j$ to zero.

Figure 3 shows the variation with both τ_{rec} and τ_{fac} of the stationary, locally stable solution with associative memory, $m \neq 0$, computed this time in both the mean-field approximation and using Monte Carlo simulation. The Monte Carlo simulation consists of iterating equations 1.1, 1.4, and 1.7 using parallel dynamics. This shows a perfect agreement between our mean-field approach above and the simulations as long as one is far from the transition, a fact that is confirmed below (in Figure 5). This is because, near τ_{rec}^*, the simulations describe hops between positive and negative m that do not compare well with the mean-field absolute value $|m|$.

The most interesting behavior is perhaps the one revealed by the phase diagram (T, τ_{fac}) in Figure 4. Here we depict a case with $U = 0.1$ in order to clearly visualize the effect of facilitation (facilitation has practically no effect for any $U > 0.5$, as shown above) and $\tau_{rec} = 3$ ms in order to compare with the situation of only depression in Pantic et al. (2002). A main result here is that for appropriate values of the working temperature T, one may force the system to undergo different types of transitions by simply varying τ_{fac}. First note that the line $\tau_{fac} = 0$ corresponds roughly to the case of static
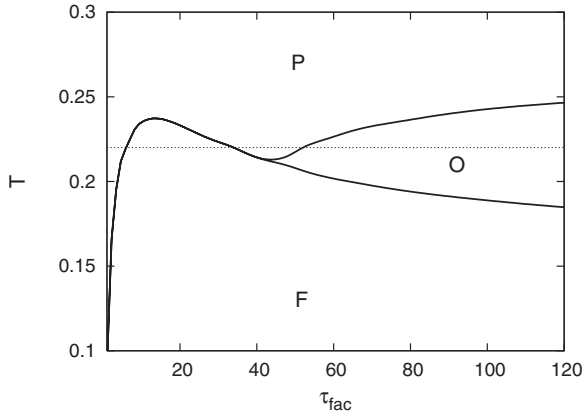
Figure 4: Phase diagram (T, τ_{fac}) for $U = 0.1$ and $\tau_{\text{rec}} = 3$ ms. This illustrates the potential high adaptability of the network to different tasks (e.g., around $T = 0.22$) by simply varying its degree of facilitation.

synapses, since τ_{rec} is very small. In this limit, the transition between the retrieval (F) and nonretrieval (P) phases is at $T = U = 0.1$. At low enough T, there is a transition between the nonretrieval (P) and retrieval phases (F) as facilitation is increased. This reveals a positive effect of facilitation on memory at low temperature and suggests improvement of the network storage capacity, which is usually measured at $T = 0$, a prediction that we have confirmed in preliminary simulations. At intermediate temperatures, for example, $T \approx 0.22$ for $U = 0.1$, the system shows no memory in the absence of facilitation, but increasing τ_{fac}, one may describe consecutive transitions to a retrieval phase (F), a disordered phase (P), and then an oscillatory phase (O). The last is associated with a new instability induced by a strong depression effect due to the further increase of facilitation. At higher T, facilitation may drive the system directly from complete disorder to an oscillatory regime.

In addition to its influence on the onset and width of the oscillatory region, the competition between depression and facilitation, described by the relation between τ_{rec} and τ_{fac}, determines the frequency of the oscillations of m. In order to study this effect, we computed the average time between the consecutive minimum and maximum of these oscillations: a half period as a function of τ_{fac} and for different values of τ_{rec}. The result is illustrated in the left graph of Figure 5. This shows that for relatively large facilitation, the frequency of the oscillations increases with the facilitation time. This means that the access of the network activity to the attractors is faster with increasing facilitation, though the system then remains near each attractor for a shorter time due to the extra depression that follows strong facilitation. However, for relatively small facilitation ($\tau_{\text{fac}} < 10$ ms), there is competition between a tendency to go to the attractors, which is favored by facilitation,
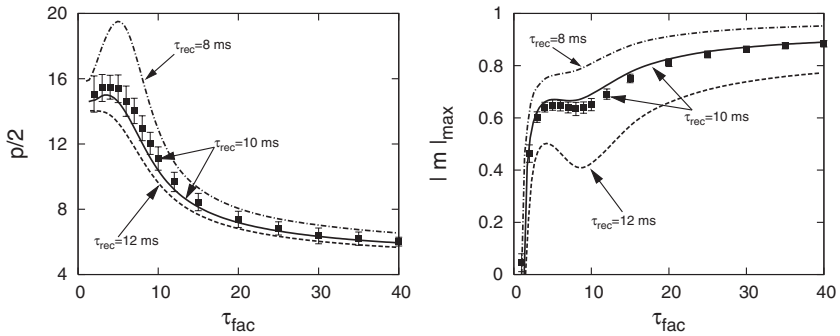
Figure 5: (Left graph) Half-period of oscillations as a function of τ_{fac}, for $U = T = 0.1$ and $P = 1$, as obtained from the mean-field solution for values of $\tau_{rec} = 12, 10, 8$ ms (curves) and from simulations (symbols) for $\tau_{rec} = 10$ ms. (Right graph) For the same conditions as in the left graph, this shows the maximum of the absolute value of m during oscillations. The simulation results in both graphs corresponding to an average over 10^3 peaks of the stationary series for m. The fact that statistical errors are small confirms the mean-field periodic behavior.

and a tendency to leave the attractor, due to depression. For a relatively week depression (e.g., $\tau_{rec} = 8$ ms), the activity tends to remain longer near the attractor, while the system takes more time to reach the attractor if facilitation is not too strong. The competition results in a large half-period for oscillations. This tendency to increase the half-period finishes when facilitation becomes very large, and then a depressing effect due to strong facilitation occurs. As a consequence, the half-period begins to decrease. This complex behavior of the half-period due to the competition between depression and facilitation washes out for strong depression, as illustrated in Figure 5 (left) for $\tau_{rec} = 12$ ms. We also computed the maximum of m during oscillations: $|m|_{max}$. This, which is depicted in the right graph of Figure 5, also increases with τ_{fac} for strong facilitation. For relatively small facilitation, again complex behavior due to the competition shows up. In this case, the effects are more evident for strong depression (see the curve $\tau_{rec} = 12$ ms in Figure 5, right), and there is a small region in which, though the access to stored information is faster (the half-period decreases), the error when one retrieves information increases ($|m|$ decreases), which is due to the fact that depression dominates.

The overall conclusion is that for relatively small facilitation, there is a nontrivial competition between depression and facilitation that, for particular values of the depression, results in nonmonotonic behavior of the half-period and maximum m during oscillations. On the other hand, not only the access to the stored information is faster under relatively large facilitation, but increasing it will then help to retrieve information with less error.
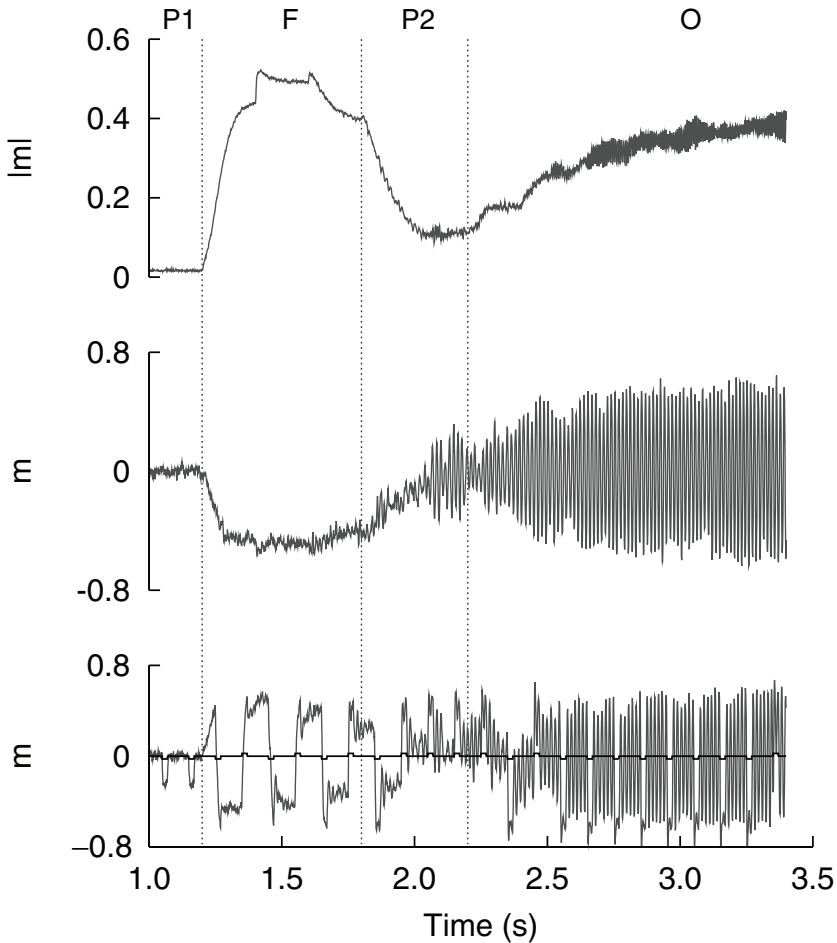
Figure 6: Time series for the overlap function, m, at $T = 0.22$ (horizontal dotted line in Figure 4) as one increases the value of τ_{fac} in order to visit the different regimes (separated here by vertical lines). The simulations started with $\tau_{\text{fac}} = 1$ at $t = 1$, and τ_{fac} was then increased by 10 units every 200 ms. The bottom graph corresponds to a case in which the system is under the action of an external stimulus (as described in the text). The middle graph depicts an individual run when the system is without any stimulus, and the top graph corresponds to the average of $|m|$ over 100 independent runs of the unperturbed system.

In order to provide more information on some aspects of the system behavior, we present in Figures 6 and 7 a detailed study of specific time series. The middle graph in Figure 6 corresponds to a simulation of the system evolution for increasing values of τ_{fac} as one describes the horizontal line
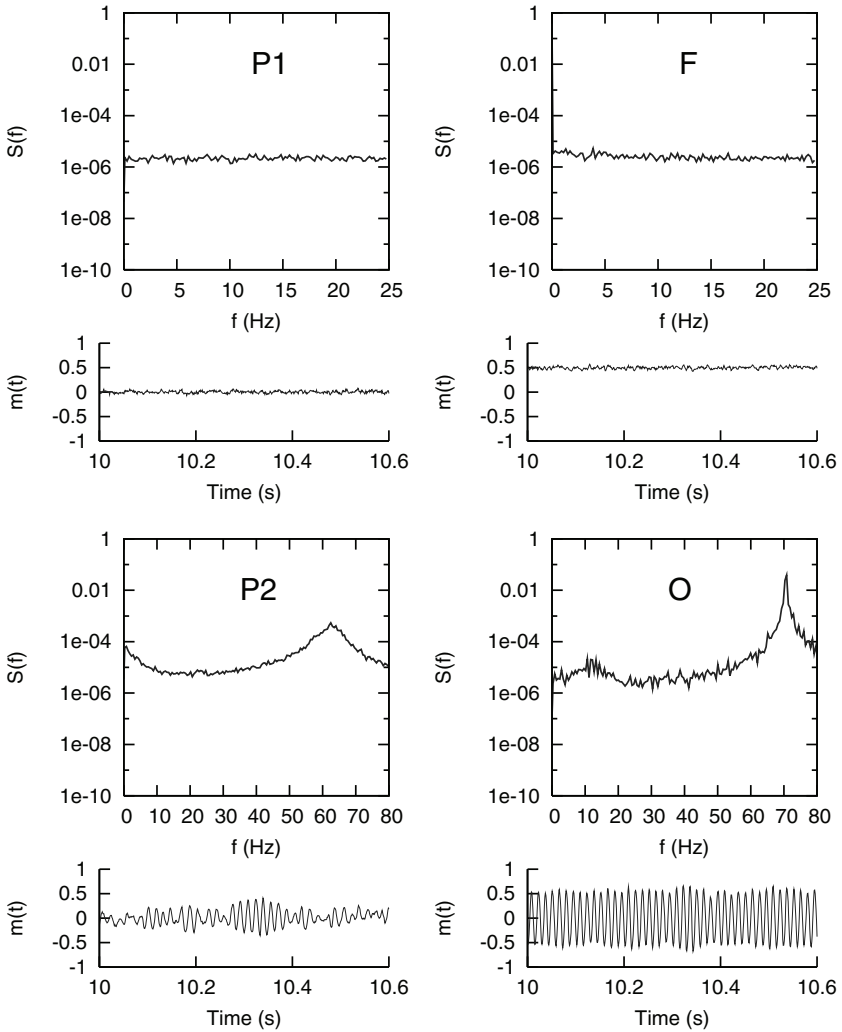
Figure 7: Spectral analysis of the cases in Figure 6. On top of each of the small panels, which show typical time series for $\tau_{fac} = 2, 20, 50,$ and 100, respectively, from top to bottom and from left to right, the square panels show the corresponding power spectra. Details of the simulations as in Figure 6.

for $T = 0.22$ in Figure 4. The system thus visits consecutively the different regions (separated by vertical lines) over time. That is, the simulation starts with the system in the stable paramagnetic phase, denoted P1 in the figure, and then successively moves by varying τ_{fac} into the stable ferromagnetic

phase F, into another paramagnetic phase, P2, and, finally, into the oscillatory phase, O.

We interpret that the observed behavior in P2 as due to competition between the facilitation mechanism, which tries to bring the system to the fixed-point attractors, and the depression mechanism, which tends to destabilize the attractors. The result is a sort of intermittent behavior in which oscillations and convergence to a fixed-point alternate in a way that resembles (but is not) chaos. The top graph in Figure 6, which corresponds to an average over independent runs, illustrates the typical behavior of the system in these simulations; the middle run depicts an individual run.

Further interesting behavior is shown in the bottom graph of Figure 6. This corresponds to an individual run in the presence of a very small and irregular external stimulus, represented by the black line around $m = 0$. This consists of an irregular series of positive and negative pulses of intensity $\pm 0.03 \, \xi^1$ and a duration of 20 ms. In addition to a great sensibility to weak inputs from the environment, this reveals that increasing facilitation tends to significantly enhance the system response.

Figure 7 shows the power spectra of typical time series such as the ones in Figure 6: describing the horizontal line for $T = 0.22$ in Figure 4 to visit the different regimes. We here plot time series $m(t)$ obtained, respectively, for $\tau_{\text{fac}} = 2$, 20, 50, and 100 and, on top of each of them, the corresponding spectra. This reveals a flat, white-noise spectrum for the P1 phase and for the stable fixed-point solution in the F regime. However, the case for the intermittent P2 phase depicts a small peak around 65 Hz. The peak is much sharper, and it occurs at 70 Hz in the oscillatory case.

4 Conclusion

We have shown that the dynamic properties of synapses have profound consequences on the behavior, and the possible functional role, of recurrent neural networks. Depending on the relative strength of depression, facilitation, and noise in the network, one observes either attraction toward one of the stored memory patterns or a nonretrieval situation in which the neurons fire largely at random in a fashion uncorrelated to the patterns, or else switching where none of the patterns is stable and the network rapidly moves between (the neighborhoods of) all of them. These three behaviors were also observed in our previous work, where we studied the role of depression only. However, the transition between the different possible phases and their nature importantly depends on the existence of competition between depression and facilitation and on the balance between these and the underlying noise.

Our analysis of the possible phases indicates a clear role for facilitation. The activity goes straight to the attractor when facilitation dominates, so that it is reached rapidly and with very small error. The system then depresses, however, which destabilizes the attractor and expedites the search

for a different one. Even more interesting is the resulting situation when facilitation is relatively small. That is, competition between depression and facilitation may then induce a critical condition in which the activity may eventually become "frozen": there is a value of frustration for each degree of depression at which the time to reach the attractor importantly increases. This behavior is less marked as depression increases; depression serves to avoid such frustration induced by intermediate values of facilitation. This is quantitatively illustrated in Figure 5.

On the other hand, under the action of only depression, we know that by avoiding too much thermal noise, the system may describe a transition from the retrieval phase to the oscillating one, and then to the nonretrieval phase as depression is increased. As shown with detail in Figures 4 and 6, the presence of facilitation may essentially modify this picture. For instance, the particular sequence of phases the system will describe depends crucially on the balance of depression, facilitation, and noise.

In summary, facilitation favors a more rapid and precise access to the stored information. It also induces a more complex situation in which competing with depression seems to allow for more diverse tasks. Interestingly, Wang et al. (2006) have recently reported the existence of depressing and facilitating synapses and their possible competition to form the basis of working memories.

Acknowledgments

References

Abbott, L. F., & Regehr, W. G. (2004). Synaptic computation. *Nature, 431*, 796–803.

Amit, D. J. (1989). *Modeling brain function: The world of attractor neural networks*. Cambridge: Cambridge University Press.

Bibitchkov, D., Herrmann, J. M., & Geisel, T. (2002). Pattern storage and processing in attractor networks with short-time synaptic dynamics. *Network: Comput. Neural Syst., 13*, 115–129.

Burnashev, N., & Rozov, A. (2005). Presynaptic Ca^{2+} dynamics, Ca^{2+} buffers and synaptic efficacy. *Cell Calcium, 37*, 489–495.

Cortes, J. M., Garrido, P. L., Marro, J., & Torres, J. J. (2004). Switching between memories in neural automata with synaptic noise. *Neurocomputing, 58–60*, 67–71.

Cortes, J. M., Torres, J. J., Marro, J., Garrido, P. L., & Kappen, H. J. (2006). Effects of fast presynaptic noise in attractor neural networks. *Neural Comput., 18*(3), 614–633.

Hopfield, J. J. (1982). Neural networks and physical systems with emergent collective computational abilities. *Proc. Natl. Acad. Sci. USA, 79*, 2554–2558.

Laurent, G., Stopfer, M., Friedrich, R. W., Rabinovich, M. I., Volkovskii, A., & Abarbanel, H. D. I. (2001). Odor encoding as an active, dynamical process: Experiments, computation and theory. *Annu. Rev. Neurosci., 24*, 263–297.

Markram, H. H., & Tsodyks, M. V. (1996). Redistribution of synaptic efficacy between pyramidal neurons. *Nature, 382*, 807–810.

Markram, H. H., Wang, Y., & Tsodyks, M. V. (1998). Differential signaling via the same axon of neocortical pyramidal neurons. *Proc. Natl. Acad. Sci. USA, 95*, 5323–5328.

Marro, J., & Dickman, R. (2005). *Nonequilibrium phase transitions in lattice models*. Cambridge: Cambridge University Press.

Marro, J., Garrido, P. L., & Torres, J. J. (1998). Effect of correlated fluctuations of synapses in the performance of neural networks. *Phys. Rev. Lett., 81*, 2827–2830.

Marro, J., Torres, J. J., & Cortes, J. M. (2007). Chaotic hopping between attractors in neural networks. *Neural Networks, 20*, 230–235.

Marro, J., Torres, J. J., Cortes, J. M., & Wemmenhove, B. (2006). *Sensitivity, itinerancy and chaos in partly-synchronized weighted networks*. Manuscript submitted for publication.

Mazor, O., & Laurent, G. (2005). Transient dynamics versus fixed points in odor representations by locust antennal lobe projection neurons. *Neuron, 48*, 661–673.

Pantic, L., Torres, J. J., Kappen, H. J., & Gielen, S. C. A. M. (2002). Associative memory with dynamic synapses. *Neural Comput., 14*, 2903–2923.

Peretto, P. (1992). *An introduction to the modeling of neural networks*. Cambridge: Cambridge University Press.

Romani, S., Amit, D. J., & Mongillo, G. (2006). Mean-field analysis of selective persistent activity in presence of short-term synaptic depression. *J. Comput. Neurosci., 20*, 201–217.

Thomson, A. M., & Deuchars, J. (1994). Temporal and spatial properties of local circuits in neocortex. *Trends Neurosci., 17*, 119–126.

Torres, J. J., Marro, J., Garrido, P. L., Cortes, J. M., Ramos, F., & Munoz, M. A. (2005). Effects of static and dynamic disorder on the performance of neural automata. *Biophysical Chemistry, 115*, 285–288.

Torres, J. J., Pantic, L., & Kappen, H. J. (2002). Storage capacity of attractor neural networks with depressing synapses. *Phys. Rev. E., 66*, 061910.

Tsodyks, M. V., & Markram, H. H. (1997). The neural code between neocortical pyramidal neurons depends on neurotransmitter release probability. *Proc. Natl. Acad. Sci. USA, 94*, 719–723.

Tsodyks, M., Pawelzik, K., & Markram, H. (1998). Neural networks with dynamic synapses. *Neural Comput., 10*, 821–835.

Wang, Y., Markram, H., Goodman, P. H., Berger, T. K., Ma, J., & Goldman-Rakic, P. S. (2006). Heterogeneity in the pyramidal network of the medial prefrontal cortex. *Nature Neurosci., 9*, 534–542.

Zucker, R. S., & Regehr, W. G. (2002). Short–time synaptic plasticity. *Annu. Rev. Physiol., 64*, 355–405.